

# Wettabilities of Self-Assembled Monolayers Generated from CF<sub>3</sub>-Terminated Alkanethiols on Gold

Yasuhiro F. Miura,<sup>†</sup> Mitsuru Takenaga,<sup>‡</sup> Thomas Koini,<sup>§</sup> Michael Graupe, Nupur Garg, Robert L. Graham, Jr.,<sup>||</sup> and T. Randall Lee\*

Department of Chemistry, University of Houston, Houston, Texas 77204-5641

Received February 6, 1998

Self-assembled monolayers of terminally fluorinated alkanethiols, CF<sub>3</sub>(CH<sub>2</sub>)<sub>n</sub>SH with  $n = 9–15$ , and their nonfluorinated analogues, CH<sub>3</sub>(CH<sub>2</sub>)<sub>n</sub>SH with  $n = 9–15$ , were prepared by adsorption from solution onto evaporated gold. The monolayers were characterized by contact angle goniometry, ellipsometry, and X-ray photoelectron spectroscopy. The analyses indicate that the CF<sub>3</sub>-terminated alkanethiols generate terminally fluorinated monolayers that are well-ordered, particularly when the chain lengths consist of 12 or more carbon atoms. Comparison of CF<sub>3</sub>-terminated films to CH<sub>3</sub>-terminated films of similar length reveals that terminal fluorination of the surface leads to an overall decrease in the surface tension of the films. This decrease arises from a relatively large decrease in the dispersive component of the surface tension upon the introduction of fluorine. Surprisingly, terminal fluorination also leads to a small but significant increase in the nondispersive component(s) of the surface tension. The origin of these opposing effects is discussed.

## Introduction

Fluorinated organic materials have drawn considerable fundamental and technological interest because of their extremely low wettabilities and surface energies.<sup>1</sup> In pioneering work more than 35 years ago, Zisman et al. examined the wettabilities of fluorinated organic thin films generated by the adsorption of fluorinated alkanic acids and alkylamines on metal surfaces.<sup>2–4</sup> Although these studies sought to provide a systematic exploration of the differences (with regard to molecular size and interfacial forces) between fluorinated films and those derived from hydrocarbons, the limited reproducibility and characterization of these early films hindered in many cases the establishment of firm conclusions.

More recently, the adsorption of alkanethiols onto gold has been shown to provide a convenient route to self-assembled monolayer (SAM) films that are highly ordered and well-defined.<sup>5</sup> Alkanethiols that are predominantly fluorinated can also be used to generate high-quality films.<sup>6–9</sup> The larger van der Waals radii of the fluorocarbon chains lead to a lower packing density than that observed for analogous hydrocarbon chains.<sup>6</sup> For example,

fluorinated SAMs generated from CF<sub>3</sub>(CF<sub>2</sub>)<sub>7</sub>(CH<sub>2</sub>)<sub>2</sub>SH on Au(111) exhibit a p(2 × 2) structure at 95% bulk density,<sup>7,8</sup> and films generated from CF<sub>3</sub>(CF<sub>2</sub>)<sub>n</sub>(CH<sub>2</sub>)<sub>2</sub>SH ( $n = 5, 7, 11$ ) on Au(111) exhibit a packing density of at most commensurate c(7 × 7).<sup>9</sup> The respective structures show packing densities that are 12% and 22% smaller than those of purely hydrocarbon-based SAMs.

In contrast to these earlier studies, our research explores the interfacial properties of a series of SAMs on gold generated from partially fluorinated alkanethiols, where the degree of fluorination is progressively increased from zero.<sup>10</sup> In the present study, we compare the properties of SAMs derived from  $\omega, \omega, \omega$ -trifluoromethylalkaneithiols (CF<sub>3</sub>(CH<sub>2</sub>)<sub>n</sub>SH, where  $n = 9–15$ ) to those of SAMs derived from the corresponding simple alkanethiols (CH<sub>3</sub>(CH<sub>2</sub>)<sub>n</sub>SH, where  $n = 9–15$ ). Analysis of the new SAMs by contact angle goniometry, ellipsometry, and X-ray photoelectron spectroscopy indicates that all of the partially fluorinated alkanethiols generate analogous CF<sub>3</sub>-terminated surfaces, which are supported by the well-organized chain structures characteristic of SAMs generated from the simple alkanethiols. An unexpected trend in the wettabilities was, however, observed: the CF<sub>3</sub>-terminated SAMs were less wettable by hexadecane and methylene iodide, but surprisingly more wettable by water and glycerol than were the CH<sub>3</sub>-terminated SAMs.

## Experimental Section

**Materials and Methods.** The liquids used for the contact angle measurements (hexadecane, methylene iodide, glycerol, and water) were of the highest purity available from Aldrich Chemical Co. and were used without further purification. The simple alkanethiols used to generate the hydrocarbon SAMs were either commercially available or synthesized using unexceptional procedures. The  $\omega, \omega, \omega$ -trifluoromethylalkaneithiols were synthesized using an approach developed in our laboratories; the details of the synthesis and characterization are described elsewhere.<sup>11</sup> The purity of all thiols was >99% as judged by integration of the corresponding nuclear magnetic resonance

\* To whom correspondence should be addressed. E-mail: trlee@uh.edu.

<sup>†</sup> Present address: Toei University of Yokohama, Yokohama, Kanagawa, Japan.

<sup>‡</sup> On leave from: Science University of Tokyo in Yamaguchi, Yamaguchi, Japan.

<sup>§</sup> Erwin Schrödinger Postdoctoral Fellow of the FWF (Austria).

<sup>||</sup> Materials Research Science & Engineering Center, Harvard University, Cambridge, MA.

(1) Garbassi, F.; Morroca, M.; Occhiello, E. *Polymer Surfaces*; Wiley: Chichester, 1994.

(2) Hare, E. F.; Shafrin, E. G.; Zisman, W. A. *J. Phys. Chem.* **1954**, *58*, 236.

(3) Shafrin, E. G.; Zisman, W. A. *J. Phys. Chem.* **1957**, *61*, 1046.

(4) Shafrin, E. G.; Zisman, W. A. *J. Phys. Chem.* **1962**, *66*, 740.

(5) For a recent review, see: Ulman, A. *Chem. Rev.* **1996**, *96*, 1533.

(6) Ulman, A.; Eilers, J. E.; Tillman, N. *Langmuir* **1989**, *5*, 1147.

(7) Alves, C. A.; Porter, M. D. *Langmuir* **1993**, *9*, 3507.

(8) Porter, M. D.; Bright, T. B.; Allara, D. L.; Chidsey, C. E. D. *J. Am. Chem. Soc.* **1987**, *109*, 3559.

(9) Liu, G.-Y.; Fenter, P.; Chidsey, C. E. D.; Ogletree, D. F.; Eisenberger, P.; Salmeron, M. *J. Chem. Phys.* **1994**, *101*, 4301.

(10) Kim, H. I.; Koini, T.; Lee, T. R.; Perry, S. S. *Langmuir* **1997**, *13*, 7192.

spectra ( $^1\text{H NMR}$ , 300 MHz). Refractive indices of all thiols were measured using a Bausch & Lomb refractometer operated at 24 °C ( $n_D^{24}$ ).

**Preparation of SAMs.** The surfaces of gold were prepared by evaporation of ca. 2000 Å of gold onto silicon (100) wafers that were precoated with ca. 100 Å of chromium to promote adhesion. SAMs were prepared by immersing small pieces of the freshly prepared gold-coated wafers in deoxygenated ethanolic solutions containing the appropriate thiols in 1 mM concentrations. The gold slides were allowed to remain in the ethanolic solution at ambient temperature for 24 h. After removal from solution, the slides were rinsed thoroughly with ethanol; the ethanol was then removed by passing a vigorous stream of nitrogen over the slide.

**Characterization of SAMs.** The thicknesses of the films were measured with a Rudolph Auto EL III ellipsometer, which employs a He–Ne laser beam (632.8 nm) at an angle of incidence of 70°. For all films, a refractive index of  $n = 1.45$  was assumed. To determine the precision, we performed at least 10 measurements of thickness for each type of film. For a given set of measurements, the values were typically reproducible to within  $\pm 1$  Å. The atomic composition of the films was determined by X-ray photoelectron spectroscopy (XPS) using a Surface Science SSX-100 spectrometer with a monochromatized Al K $\alpha$  source.

Advancing and receding contact angles were measured using a Ramé–Hart model 100 contact angle goniometer. Contacting liquids were applied (for advancing angles,  $\theta_a$ ) and withdrawn (for receding angles,  $\theta_r$ ) using a Matrix Technologies micro-Electrapette 25 operated at the slowest possible speed (ca. 1  $\mu\text{L/s}$ ). Two measurements of the contact angle at 293 K and ambient relative humidity were performed on opposite edges of at least three drops (ca. 3 mm diameter) with the pipet tip touching the drops. The contact angles were typically reproducible to within  $\pm 1^\circ$ . Four types of pure test liquids were used: hexadecane ( $\text{C}_{16}\text{H}_{34}$ , HD), methylene iodide ( $\text{CH}_2\text{I}_2$ , MI), glycerol ( $\text{C}_3\text{H}_5(\text{OH})_3$ , GL) and distilled water ( $\text{H}_2\text{O}$ , W). The advancing contact angle  $\theta_a$  was used for calculation of the surface tensions because of ready comparison with published data.

**Estimation of Surface Tensions.** The surface tensions of the SAMs were estimated from the contact angle data utilizing a separation method proposed by van Oss, Chaudhury, and Good.<sup>12,13</sup> This method yields the solid surface tension  $\gamma_S$  as a summation of the respective surface tension components  $\gamma_S^{\text{LW}}$  and  $\gamma_S^{\text{AB}}$  (i.e.,  $\gamma_S = \gamma_S^{\text{LW}} + \gamma_S^{\text{AB}}$ ), based on Lifshitz–van der Waals (or dispersive interactions) and acid–base (or hydrogen bonding interactions), respectively. The term  $\gamma^{\text{AB}}$  is a combination of the asymmetric components  $\gamma^+$  (acid or electron acceptor interactions) and  $\gamma^-$  (base or electron donor interactions):  $\gamma^{\text{AB}} = 2(\gamma^+ \gamma^-)^{1/2}$ . The relationship between the equilibrium contact angle  $\theta$  and the surface tension components of liquids and solids is given by the modified Young–Dupré equation (eq 1)<sup>14</sup>

$$(1 + \cos \theta) \gamma_L = 2(\gamma_S^{\text{LW}} \gamma_L^{\text{LW}})^{1/2} + 2(\gamma_S^+ \gamma_L^-)^{1/2} + 2(\gamma_S^- \gamma_L^+)^{1/2} \quad (1)$$

The term  $\gamma_L$  is the surface tension of liquids against air or vapor; addition of the subscript “L” denotes the surface tension components of the test liquids. The geometric mean is assumed in the solid–liquid interfacial tensions. In our case, the calculations were performed using the  $\theta_a$  data obtained with hexadecane (HD), methylene iodide (MI), glycerol (GL), and water (W). The respective values of the liquid surface tensions are shown in Table 1.

## Results and Discussion

As a first step, it will be useful to establish an abbreviated nomenclature for the SAMs under consid-

(11) Graupe, M.; Koini, T.; Wang, V. Y.; Nassif, G. M.; Colorado, R., Jr.; Villazana, R. J.; Miura, Y. F.; Shmakova, O. E.; Lee, T. R. *J. Fluorine Chem.*, in press.

(12) van Oss, C. J.; Chaudhury, M. K.; Good, R. J. *Adv. Colloid Interface Sci.* **1987**, *28*, 35.

(13) For an independent summary and analysis of this empirical method, please see: Lee, L. H. *Langmuir* **1996**, *12*, 1681.

(14) van Oss, C. J. *Interfacial Forces in Aqueous Media*; Marcel Dekker: New York, 1994; p 20.

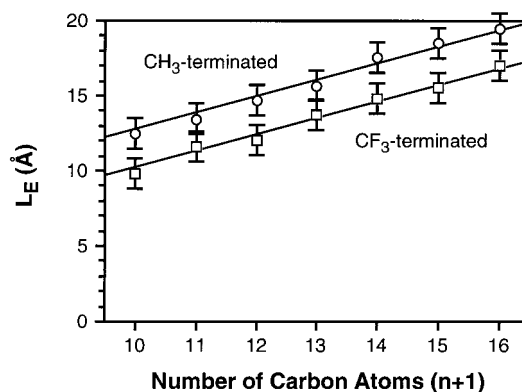


**Figure 1.** Ellipsometric thicknesses  $L_E$  of the  $\text{CH}_3$ -terminated SAMs (circles) and the  $\text{CF}_3$ -terminated SAMs (squares) as a function of the number of carbon atoms in the chain ( $n + 1$ ). Straight lines are  $L_E$  (in Å) =  $1.27 \cos(30^\circ)n + 2.8$  (upper) or  $0.3$  (lower). The error bars assume an uncertainty of  $\pm 1$  Å in the measured values of ellipsometric thickness.

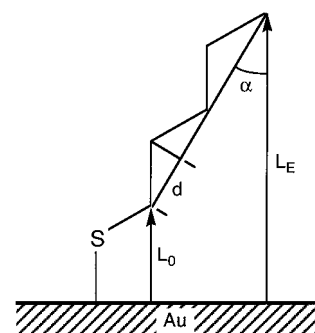


**Figure 2.** Illustration of the relationship between the components of the equation  $L_E = d \cos(\alpha)n + L_0$ .

**Table 1.** Values of Surface Tension for the Test Liquids at 293 K in  $\text{mJ m}^{-2}$ <sup>13</sup>

liquid	$\gamma_L$	$\gamma_L^{\text{LW}}$	$\gamma_L^+$	$\gamma_L^-$
hexadecane	27.5	27.5	0	0
methylene iodide	50.8	50.8	0	0
glycerol	64	34	5.3	42.5
water	72.8	21.8	34.2	19

eration here. SAMs generated from  $\text{CF}_3(\text{CH}_2)_n\text{SH}$  with  $n = 9$ –15 will be denoted as F10–F16, respectively; their hydrocarbon analogues,  $\text{CH}_3(\text{CH}_2)_n\text{SH}$  with  $n = 9$ –15, will be denoted as H10–H16, respectively.

**Thicknesses of the Films.** Figure 1 shows the ellipsometric thicknesses ( $L_E$ ) plotted against the chain lengths for both the  $\text{CH}_3$ - and the  $\text{CF}_3$ -terminated SAMs. The observed thicknesses for the  $\text{CH}_3$ -terminated SAMs successively increase from 12.5 to 19.5 Å with increasing chain length. A similar trend is observed for the  $\text{CF}_3$ -terminated SAMs; for all chain lengths, however, the magnitudes of the thicknesses are smaller than those generated from the corresponding simple alkanethiols by an average of  $2.5 \pm 1.2$  Å.

An approximate relationship between  $L_E$  and the composition of the SAMs is also shown in Figure 1 as a linear curve having the following form:  $L_E = d \cos(\alpha)n + L_0$ , where  $d$  is the length of the projection of the C–C bond onto the main chain axis ( $d = 1.27$  Å; Figure 2),<sup>15</sup>  $\alpha$  is the mean tilt angle of the chain axis from the surface normal ( $\alpha = 30^\circ$ ),<sup>16</sup>  $n$  is the chain length defined by  $\text{CH}_3(\text{CH}_2)_n\text{SH}$ , and  $L_0$  is the intercept (i.e., the value of  $L_E$  at  $n = 0$ ). From

(15) Assuming a C–C–C bond angle of  $112^\circ$  for the polymethylene chains: Dunitz, J. D. *X-ray Analysis and the Structure of Organic Molecules*; Cornell: Ithaca, 1979; p 338.

the ellipsometric data for the CH<sub>3</sub>-terminated films, we obtain a value of  $L_0 = 2.8 \pm 0.9 \text{ \AA}$ , which represents a reasonable value for the bond length and angle of the C–S/Au interaction. For the CF<sub>3</sub>-terminated films, however, we obtain a value of  $L_0 = 0.3 \pm 0.8 \text{ \AA}$ , which seems anomalously small.

We explored the possibility that the small  $L_E$  observed for the CF<sub>3</sub>-terminated monolayers was due to the use of an inappropriately high value for the refractive index, which could give rise to an underestimate of the thicknesses of these films. We measured the refractive indices of the alkanethiols examined in this study and found the average value,  $n_D^{24} = 1.458 \pm 0.004$ ; the average value obtained for the corresponding CF<sub>3</sub>-terminated thiols was indeed lower:  $n_D^{24} = 1.431 \pm 0.009$ . The magnitude of the difference is, however, insufficient to completely account for the observed differences in the thicknesses of the two types of films.<sup>17,18</sup> Furthermore, analysis of the H13 and F13 SAMs by atomic force microscopy (AFM) revealed an indistinguishable difference in lattice spacing for the two films.<sup>10</sup> Consequently, it seems unlikely that differences in packing density are responsible for the differences in ellipsometric thickness. A remaining possibility is that a difference in tilt angle for the two types of films is giving rise to the observed differences in thickness. We are currently examining these films by infrared reflection–absorption spectroscopy (IRRAS)<sup>19,20</sup> to evaluate this possibility.

**Elemental Compositions of the Films.** Analysis of the CF<sub>3</sub>-terminated films by XPS revealed no detectable oxygen or other spurious elements (data not shown). The ratio of fluorine/gold was roughly constant over the range of chain lengths examined (F10–F13). Although we might have expected this ratio to increase with increasing chain length, the data are nevertheless consistent with a model in which all CF<sub>3</sub>-terminated alkanethiols provide similar surface coverages, exposing fluorine atoms at the interface.

**Wettabilities of the Films.** Figure 3a shows the advancing contact angle  $\theta_a$  (and  $\cos \theta_a$ ) plotted against chain length for the CH<sub>3</sub>-terminated monolayers H10–H16. The average values for  $\theta_a$  (and  $\cos \theta_a$ ) are 48° (0.67) for HD, 78° (0.21) for MI, 101.5° (–0.20) for GL, and 114.5° (–0.41) for W. For a given test liquid, the measured values are nearly constant for all chain lengths. To evaluate these measurements, published data for similar SAMs on gold with a wide range of chain lengths are readily available:  $\theta_a$  values for H12–H15 are constant within 45–48° for HD and 111–114° for W, while  $\theta_a$  for shorter chain lengths are progressively lower.<sup>21,22</sup> Similar data have been observed for SAMs formed on other metals.<sup>22</sup> In addition, there are reports of a parity (or “odd–even”) effect in the contact angle versus chain length data observed for hexadecane wetting SAMs on gold.<sup>16,23</sup> The parity effect is generally interpreted to reflect the increased

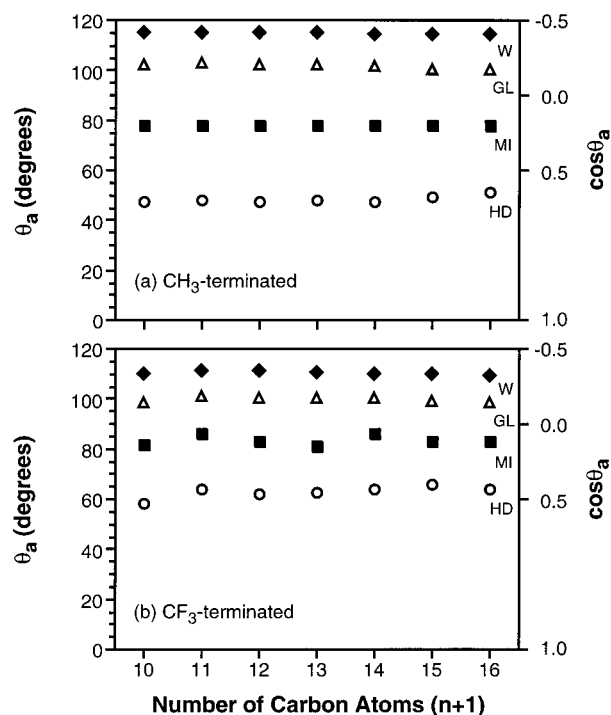


**Figure 3.** Advancing contact angles  $\theta_a$  (and  $\cos \theta_a$ ) for CH<sub>3</sub>-terminated SAMs (a) and the CF<sub>3</sub>-terminated SAMs (b) as a function of the number of carbon atoms in the chain ( $n + 1$ ). Hexadecane (HD), methylene iodide (MI), glycerol (GL), and water (W) were used as the test liquids. The contact angles were typically reproducible to within  $\pm 1^\circ$ .

wettability of methylene vs methyl groups exposed at the interface.<sup>24,25</sup> We routinely observe this effect;<sup>26</sup> in the data shown here, however, the effect is absent.<sup>27</sup> With regard to these results and the ellipsometry data above, we conclude that SAMs H10–H16 form similar well-ordered surfaces with oriented and densely packed chains.

Figure 3b shows the advancing contact angle  $\theta_a$  (and  $\cos \theta_a$ ) plotted against chain length for the CF<sub>3</sub>-terminated monolayers F10–F16. The data for F10 slightly deviate toward lower contact angles (corresponding to higher wettability) for all test liquids employed. For a given test liquid, the measured values are nearly constant for chain lengths greater than F10, and no parity effect is observed. The average values for  $\theta_a$  (and  $\cos \theta_a$ ) for F11–F16 are 64° (0.44) for HD, 84° (0.10) for MI, 100° (–0.17) for GL, and 110° (–0.34) for W. In addition, the difference in contact angle between CF<sub>3</sub>- and CH<sub>3</sub>-terminated SAMs ( $\Delta\theta_a = \theta_a^{\text{CF}_3} - \theta_a^{\text{CH}_3}$ ) is roughly constant over all chain lengths: 15° for HD, 6° for MI, –2° for GL, and –4° for W. These data indicate that the dispersive liquids are repelled more at the CF<sub>3</sub>-terminated surfaces, while the polar hydrogen-bonding liquids are repelled more at the CH<sub>3</sub>-terminated surfaces.

**Contact Angle Hysteresis.** Figure 4 shows the contact angle hysteresis,  $\Delta(\cos \theta) = |\cos \theta_a - \cos \theta_r|$ , as a function of chain length of both the CH<sub>3</sub>- and the CF<sub>3</sub>-

(16) Sellers, H.; Ulman, A.; Schnidman, Y.; Eilers, J. E. *J. Am. Chem. Soc.* **1993**, *115*, 9389.

(17) In separate studies of the ellipsometric thicknesses of chelating SAMs on gold,<sup>18</sup> we varied the assumed refractive index from 1.40 to 1.60 and found the corresponding thicknesses to decrease by only 1 Å. Since the difference in average refractive index for the alkanethiols and the CF<sub>3</sub>-terminated alkanethiols is at most 0.04, we believe that some other factor must be contributing to the observed differences in thickness ( $\Delta L_E = 2.5 \pm 1.2 \text{ \AA}$ ) for these two types of films.

(18) Garg, N.; Lee, T. R. *Langmuir*, **1998**, *14*, 3815.

(19) Allara, D. L. in *Characterization of Organic Thin Films*; Ulman, A., Ed.; Butterworth-Heinemann, Boston, 1995; pp 57–86.

(20) See also: Anderson, M. R.; Evaniak, M. N.; Zhang, M. *Langmuir* **1996**, *12*, 2327.

(21) Bain, C. D.; Troughton, E. B.; Tao, Y.-T.; Evall, J.; Whitesides, G. M.; Nuzzo, R. G. *J. Am. Chem. Soc.* **1989**, *111*, 321.

(22) Laibinis, P. E.; Whitesides, G. M.; Allara, D. L.; Tao, Y.-T.; Parikh, A. N.; Nuzzo, R. G. *J. Am. Chem. Soc.* **1991**, *113*, 7152.

(23) Chang, S.-C.; Chao, I.; Tao, Y.-T. *J. Am. Chem. Soc.* **1994**, *116*, 6792.

(24) Tao, Y.-T. *J. Am. Chem. Soc.* **1993**, *115*, 4350.

(25) Tao, Y.-T.; Lee, M.-T.; Chang, S.-C. *J. Am. Chem. Soc.* **1993**, *115*, 9547.

(26) See, for example: Graupe, M.; Koini, T.; Kim, H. I.; Garg, N.; Miura, Y. F.; Takenaga, M.; Perry, S. S.; Lee, T. R. *Colloids Surf. A*, in press.

(27) We have yet to establish the origin of this inconsistency. Empirical observations suggest, however, a variance with the quality of the underlying gold; that is, SAMs grown on only the highest quality evaporated gold appear to exhibit the parity effect.



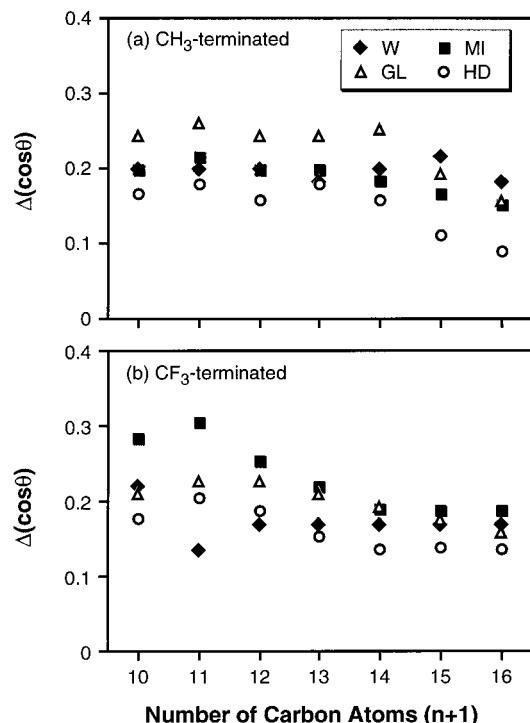


**Figure 4.** Hysteresis of contact angles  $\Delta(\cos \theta)$  for  $\text{CH}_3$ -terminated SAMs (a) and the  $\text{CF}_3$ -terminated SAMs (b) as a function of the number of carbon atoms in the chain ( $n+1$ ). Hexadecane (HD), methylene iodide (MI), glycerol (GL), and water (W) were used as the test liquids.

terminated films. These data provide a measure of the roughness or heterogeneity of the wetted surfaces.<sup>28–34</sup> For the  $\text{CH}_3$ -terminated surfaces, average values of  $\Delta(\cos \theta)$  for each test liquid are 0.15 for HD, 0.19 for MI, 0.23 for GL, and 0.20 for W. The observed values of hysteresis are comparable with those reported in the literature for SAMs of alkanethiols on gold.<sup>21,22</sup> Our data also suggest that regardless of the chain length, the surfaces of the present  $\text{CH}_3$ -terminated SAMs are equally smooth and homogeneous (although a trend toward smoother, more homogeneous surfaces could be proposed for the thickest films, H15 and H16).

The  $\text{CF}_3$ -terminated SAMs having longer chain lengths (i.e., F12–F16) exhibit qualitatively similar behavior: the average values of  $\Delta(\cos \theta)$  for all test liquids fall within the interval of 0.16–0.23. Furthermore, with the exception of W, the contact angle hystereses show a progressive decrease with increasing chain length. A deviation from this trend is, however, observed for the shorter  $\text{CF}_3$ -terminated SAMs, F10 and F11. This behavior might result from a transition to rougher, more heterogeneous surfaces for the shorter chain lengths.<sup>28,30</sup> An increase in the hysteresis of the  $\text{CF}_3$ -terminated SAMs at shorter chain lengths might be attributed to disorder imposed by the larger terminal  $\text{CF}_3$  group.<sup>35,36</sup> This effect might be overcome at the longer chain lengths due to the increased

van der Waals interactions between the  $\text{CH}_2$  groups forming the backbones, which would afford stronger interchain packing and thus more highly ordered films.<sup>21</sup>

For the model of surface heterogeneity proposed by Johnson and Dettre,<sup>32</sup> the contact angle hysteresis is controlled by (1) the energies of two adjacent configurations where the drop is at a metastable equilibrium and (2) the energy barrier between those two configurations. It follows that a larger  $\Delta(\cos \theta)$  should correlate with greater work required to move a drop from one position of a metastable equilibrium to a position of unstable equilibrium and ultimately again to a position of metastable equilibrium. If the SAMs generated by shorter chains are indeed less ordered than those with longer chains, this disorder might manifest itself in the formation of a large number of domains and the corresponding borders between them.<sup>7</sup> In the Johnson and Dettre model (based on work by Pease<sup>37</sup>),<sup>32</sup> the advancing angles are most closely associated with low-energy regions of the surface, while the receding angles are most closely associated with high-energy regions. If the boundaries and steps between domains can be characterized as higher energy regions compared to lower energy flat regions, the observed hystereses could indicate the existence of progressive border formation for decreasing chain lengths.<sup>38</sup>

Since the handling and preparation (including the fabrication of the Au substrates) of all SAMs carried out under similar conditions, we assume that the hysteresis effects imposed by any adsorbed impurities or contaminants should be similar for all films. It is also known that the surfaces of low-energy SAMs are generally insensitive to contaminants.<sup>21</sup> Additionally, the XPS analyses of the  $\text{CF}_3$ -terminated SAMs showed no detectable contamination.

**Surface Tensions of the Films.** Figure 5a shows the estimated surface tensions  $\gamma_s$ ,  $\gamma_s^{\text{LW}}$ , and  $\gamma_s^{\text{AB}}$  plotted against the chain lengths of the  $\text{CH}_3$ -terminated films.<sup>12,13</sup> The estimated values of  $\gamma_s$  are consistent from sample to sample and represent an exclusive contribution from  $\gamma_s^{\text{LW}}$ . The average values in  $\text{mJ m}^{-2}$  for all samples are given in Table 2; values of surface tension were calculated using HD and MI separately as the dispersive test liquids.<sup>12,13</sup> All of the  $\text{CH}_3$ -terminated SAMs appear to consist of densely packed chains with similar low-energy methyl-terminated surfaces.<sup>39</sup>

As shown in Figure 5b, the estimated surface tensions of the  $\text{CF}_3$ -terminated SAMs remain more or less constant for the chain lengths F11–F16. Deviations in the wettability of F10, perhaps due to disorder in the film, have been noted above. Overall, the estimated surface tensions for the terminally fluorinated SAMs consist of a large contribution from  $\gamma_s^{\text{LW}}$  and a small but significant contribution from  $\gamma_s^{\text{AB}}$  (see also Table 2). It is possible that the observed  $\gamma_s^{\text{AB}}$  component arises from hydrogen bonding between the  $\text{CF}_3$  groups and the polar liquids. The energy of hydrogen bonds of the type  $\text{C}\cdots\text{H}\cdots\text{O}$  has been estimated to be as high as 2.4 kcal/mol.<sup>40</sup> Furthermore, it seems plausible that optimal  $\text{C}\cdots\text{H}\cdots\text{O}$  bonds

(28) de Gennes, P. G. *Rev. Mod. Phys.* **1985**, *57*, 827.

(29) Joanny, J. F.; de Gennes, P. G. *J. Chem. Phys.* **1984**, *81*, 552.

(30) Johnson, R. E., Jr.; Dettre, R. H. In *Contact Angle, Wettability, and Adhesion*; Fowkes, F. M., Ed.; Advances in Chemistry 43; American Chemical Society: Washington, DC, 1964; pp 112 and 136.

(31) Eick, J. D.; Neumann, A. W. *J. Colloid Interface Sci.* **1975**, *53*, 235.

(32) Johnson, R. E., Jr.; Dettre, R. H. *J. Phys. Chem.* **1964**, *68*, 1744.

(33) Neumann, A. W.; Good, R. J. *J. Colloid Interface Sci.* **1972**, *38*, 341.

(34) Wu, S. *Polymer Interface and Adhesion*; Marcel Dekker: New York, 1982.

(35) Seebach, D. *Angew. Chem., Int. Ed. Engl.* **1990**, *29*, 1320.

(36) Analysis of SAMs H13 and F13 by AFM indicates that although both films are highly ordered with indistinguishable lattice parameters, the F13 film is slightly more disordered (see ref 10).

(37) Pease, D. C. *J. Phys. Chem.* **1945**, *49*, 107.

(38) This interpretation is consistent with alternative models of hysteresis in which penetration of the wetting liquid into surface defects leaves a more wettable surface for the receding angle to sense: Johnson, R. E., Jr.; Dettre, R. H. In *Wettability and Contact Angles*; Matijevic, F. M., Ed.; Surface and Colloid Science; Wiley: New York, 1969.

(39) Chaudhury, M. K. *Mater. Sci., and Eng.* **1996**, *R16*, 97.

(40) Howard, J. A. K.; Hoy, V. J.; O'Hagan, D.; Smith, G. T. *Tetrahedron* **1996**, *52*, 12613.

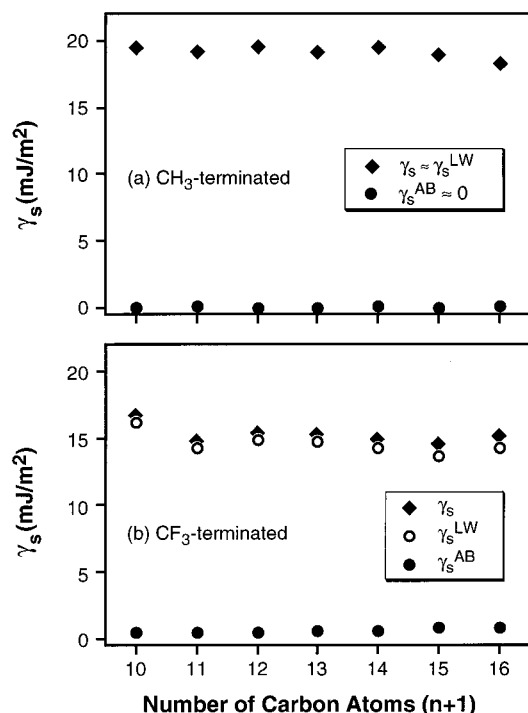


**Figure 5.** Surface tensions  $\gamma_s$ ,  $\gamma_s^{LW}$ , and  $\gamma_s^{AB}$  for CH<sub>3</sub>-terminated SAMs (a) and the CF<sub>3</sub>-terminated SAMs (b) as a function of the number of carbon atoms in the chain ( $n + 1$ ). Hexadecane (HD), methylene iodide (MI), glycerol (GL), and water (W) were used as the test liquids.

**Table 2.** Average Surface Tensions for CH<sub>3</sub>- and CF<sub>3</sub>-Terminated SAMs at 293 K in mJ m<sup>-2</sup>

SAMs	$\gamma_s$	$\gamma_s^{LW}$	$\gamma_s^{AB}$	$\gamma_s^+$	$\gamma_s^-$
H10-H16 <sup>a</sup>	19.1 ± 0.4	19.1 ± 0.4	0	0	0
H10-H16 <sup>b</sup>	18.5 ± 0.5	18.5 ± 0.5	0	0	0
F11-F16 <sup>a</sup>	15.0 ± 0.4	14.3 ± 0.4	0.7 ± 0.2	0.2 ± 0.1	0.5 ± 0.1
F11-F16 <sup>b</sup>	16.0 ± 0.8	15.5 ± 0.8	0.5 ± 0.2	0.1 ± 0.05	0.5 ± 0.1

<sup>a</sup> Calculated using HD as the dispersive test liquid. <sup>b</sup> Calculated using MI as the dispersive test liquid. The uncertainties were estimated by propagating an uncertainty of  $\pm 1^\circ$  in measurements of contact angle.

could form at the interface of CF<sub>3</sub>-terminated SAMs with polar test liquids such as glycerol and water.

Perfluorinated surfaces, however, typically exhibit little or no contribution from  $\gamma_s^{AB}$ .<sup>13</sup> In addition, perfluorinated surfaces are typically wet less well than hydrocarbon surfaces by all types of liquids, including those that are polar and exhibit hydrogen bonding.<sup>41</sup> Consequently, it is likely that we are observing a different type of phenomenon. We propose that the unusual wettabilities result from the CF<sub>3</sub>-CH<sub>2</sub> dipoles present at the surface of these films.<sup>42</sup> In this interpretation, the polar liquids more readily wet the CF<sub>3</sub>-terminated surfaces (compared to the CH<sub>3</sub>-terminated surfaces) because of the interaction between the polar liquids and the surface dipoles. We are currently exploring this phenomenon in greater depth.

The fact that  $\gamma_s$  for the CF<sub>3</sub>-terminated surfaces (ca. 15 mJ m<sup>-2</sup>) is markedly smaller than that for the CH<sub>3</sub>-terminated surfaces (ca. 19 mJ m<sup>-2</sup>) is due predominantly to differences in the dispersive component of the surface tension,  $\gamma_s^{LW}$  (see Table 2). Consequently, any polar

contribution to the surface tensions of the CF<sub>3</sub>-terminated films appears to be more than compensated by the weak dispersive interactions in these films. Although it is well established that the dispersive forces for fluorocarbon interfaces are substantially weaker than those for analogous hydrocarbon interfaces,<sup>43</sup> the results presented here are tempered by the perhaps inappropriate use of hydrocarbon liquids to evaluate (via contact angle measurements) the energies of fluorocarbon surfaces.<sup>44,45</sup>

## Conclusions

The composition, thickness, and wettability of terminally fluorinated SAMs prepared from CF<sub>3</sub>(CH<sub>2</sub>)<sub>*n*</sub>SH (where  $n = 9-15$ ) were examined and compared to their nonfluorinated analogues. While the terminally fluorinated SAMs appear to be highly oriented and densely packed like their hydrocarbon predecessors, several differences in the surface properties were observed. First, the ellipsometric thicknesses of the CF<sub>3</sub>-terminated SAMs were less than those of the corresponding CH<sub>3</sub>-terminated SAMs of identical chain length. This discrepancy arises at least in part from the use of an anomalously high value of the refractive index in the analysis of the CF<sub>3</sub>-terminated SAMs. Second, the contact angle hysteresis measured using a variety of test liquids was similar for all SAMs except those that were terminally fluorinated and of shorter chain length (i.e., F10 and F11); for these SAMs, the hysteresis was noticeably higher. We attribute this effect to greater disorder in the shorter terminally fluorinated SAMs, where the interchain van der Waals stabilization is apparently overcome by repulsion between the relatively large fluorinated  $\omega$ -termini. Third, the CF<sub>3</sub>-terminated SAMs exhibited significantly lower surface energies than the CH<sub>3</sub>-terminated SAMs despite the presence of a significant positive contribution from  $\gamma_s^{AB}$ , which is zero for the CH<sub>3</sub>-terminated SAMs. Although  $\gamma_s^{AB}$  is usually taken to represent Lewis acid-base (or hydrogen-bonding) interactions between contacting media, we propose that (at least in this system) the positive values of  $\gamma_s^{AB}$  instead represent attractive polar interactions between the contacting polar liquids and the surface CF<sub>3</sub>-CH<sub>2</sub> dipoles of the terminally fluorinated SAMs. The low surface energies of the CF<sub>3</sub>-terminated SAMs appear, however, to be predominantly influenced by the weakness of the dispersive interactions in these films.

**Acknowledgment.** We thank the University of Houston Energy Laboratory for providing seed funding and the National Science Foundation (DMR-9700662) for current support of this research. Acknowledgment is made to the donors of the Petroleum Research Fund, administered by the ACS, for partial support of this research (ACS-PRF 30614-G5). We thank Dr. Yuan Z. Lu for assistance with the XPS measurements, which were provided with support from the Harvard University MRSEC/NSF under Award Number DMR-94000396. We thank Mr. Lon Porter for assistance with the statistical analyses. We also thank Professors Manoj Chaudhury and Paul Laibinis for many helpful discussions.

LA980154G

(41) See, for example, ref 21.

(42) The concept that a surface CF<sub>3</sub>-CH<sub>2</sub> dipole might influence wettability was originally proposed by Shafrin and Zisman (ref 3). Erratic wettability data and the dual proposal of H-bonding to the CF<sub>3</sub> group, however, greatly weakened the proposal.

(43) See, for example, Chapter 5 of ref 34.

(44) Chaudhury, M. K.; Whitesides, G. M. *Science* **1992**, *256*, 1539.

(45) Drummond, C. D.; Georgakilas, G.; Chan, D. Y. C. *Langmuir* **1996**, *12*, 2617. Drummond, C. D.; Chan, D. Y. C. *Langmuir* **1997**, *13*, 2617.